Werner states and the two-spinors Heisenberg anti-ferromagnet

J. Batle[1], M. Casas[1], A. Plastino[3,4], and A. R. Plastino[2,3,5]
[1] *Departament de Física, Universitat de les Illes Balears and IMEDEA-CSIC, 07122 Palma de Mallorca, Spain*
[2] *Faculty of Astronomy and Geophysics, National University La Plata, C.C. 727, 1900 La Plata*
[3] *Argentina's National Research Council (CONICET)*
[4] *Department of Physics, National University La Plata, C.C. 727, 1900 La Plata, Argentina*
[5] *Department of Physics, University of Pretoria, 0002 Pretoria, South Africa*

We ascertain, following ideas of Arnesen, Bose, and Vedral concerning thermal entanglement [Phys. Rev. Lett. **87** (2001) 017901] and using the statistical tool called *entropic non-triviality* [Lamberti, Martin, Plastino, and Rosso, Physica A **334** (2004) 119], that there is a one to one correspondence between (i) the mixing coefficient x of a Werner state, on the one hand, and (ii) the temperature T of the one-dimensional Heisenberg two-spin chain with a magnetic field B along the $z-$axis, on the other one. This is true for each value of B below a certain critical value B_c. The pertinent mapping depends on the particular $B-$value one selects within such a range.
Pacs: 03.67.-a; 89.70.+c; 03.65.-w; 02.50.-r

I. INTRODUCTION

Entanglement is one of the most fundamental issues of quantum theory [1–6] and the so-called Werner states [7] have played a distinguished role in the unravelling of the fascinating issues at play (see, for instance, [8–10]). The Werner density matrix reads

$$\rho_W \;=\; x|\Phi^+\rangle\langle\Phi^+| \;+\; \frac{1-x}{4}I, \tag{1}$$

where $|\Phi^+\rangle$ is a Bell state (maximally entangled). The state (1) is separable (unentangled) for the mixing coefficient $x \leq 1/3$ [7]. For $x > 1/3$ they are entangled and violate the CHSH inequality for $x > 1/\sqrt{2}$ [8–10]. We see that Werner states are mixtures of noise and a maximally entangled state, and therefore, for values of the mixing parameter $x > 1/3$ they are entangled, violate the CHSH inequality and exhibit nonclassical features [8–10].
Following the interesting work of Arnesen *et al.* [11], we concern ourselves with the issue of *thermal entanglement* and consider the Hamiltonian for the 1D Heisenberg spin chain with a magnetic field of intensity B along the z-axis

$$H \;=\; \sum_{i=1}^{N}(B\sigma_z^i \;+\; J_H\vec{\sigma}^i\,\vec{\sigma}^{i+1}), \tag{2}$$

where $\sigma^i_{x,y,z}$ stand for the Pauli matrices associated with spin i and periodic boundary conditions are imposed ($\sigma_\mu^{N+1} = \sigma_\mu^1$). J_H gives the strength of the spin-spin repulsive interaction (only the anti-ferromagnetic ($J_H > 0$) instance is discussed). If we limit ourselves to the case $N = 2$, we will be dealing with two spinors, i.e., with a two-qubits system. For "thermal equilibrium" we should consider [11] the thermal state

$$\rho(T) = \frac{\exp(-\frac{H}{k_BT})}{Z(T)}, \tag{3}$$

with $Z(T)$ the partition function. Expressing both H and $\rho(T)$ in the computational basis $|00\rangle, |01\rangle, |10\rangle, |11\rangle$ we obtain

$$H = \begin{pmatrix} 2J_H + 2B & 0 & 0 & 0 \\ 0 & -2J_H & 4J_H & 0 \\ 0 & 4J_H & -2J_H & 0 \\ 0 & 0 & 0 & 2J_H - 2B \end{pmatrix}. \tag{4}$$

After defining, for convenience's sake,
$e_{wmy} = \exp\,(-2w - 2y)$;
$e_{wp} = \exp\,(-2w) + \exp\,(6w)$;
$e_{wm} = \exp\,(-2w) - \exp\,(6w)$;
$e_{wpy} = \exp\,(-2w + 2y)$,
with $w = J_H/k_BT$ and $y = B/k_BT$, we also get

$$\rho(T) = \frac{1}{Z(T)}\begin{pmatrix} e_{wmy} & 0 & 0 & 0 \\ 0 & e_{wp}/2 & e_{wm}/2 & 0 \\ 0 & e_{wm}/2 & e_{wp}/2 & 0 \\ 0 & 0 & 0 & e_{wpy} \end{pmatrix}, \tag{5}$$

The concurrence of $\rho(T)$ reads [11]

$$\begin{aligned} C &= 0; && \text{for } \mathrm{T} \geq \mathrm{T_c}, \\ C &= \frac{e^{8w} - 3}{1 + e^{-2y} + e^{2y} + e^{8w}}; && \text{for } \mathrm{T} < \mathrm{T_c}, \end{aligned} \tag{6}$$

For our purposes we must emphasize that there is no entanglement beyond a certain critical temperature $T_c = 8J_H/(k_B \ln 3)$ [11]. Clearly, the temperature plays a sort of "mixedness-role", since it is well-known that entanglement vanishes for a high enough degree of mixing. Notice that T_c is independent of B and thus an intrinsic structural property that depends (linearly) just on the interaction strength J_H. For strong enough coupling strengths we encounter non null entanglement for a wide range of temperature values.
Also, there is a change in the structure of the ground state of hamiltonian (2) when the magnetic field reaches the critical value $B_c = 4J_H$.

Remarkably, the Werner states (1) and the thermal states (3) of the 1D Heisenberg model for $N = 2$ can be related by a one to one correspondence between the mixing parameter x and the temperature T for each value of $B \leq B_c$. By means of this relation we explore for both states the evolution of the entanglement of formation as a function of the temperature.

The paper is organized as follows: In Section II we introduce the entropic non triviality measure based on the Jensen-Shannon divergence, which is the basic tool that provides a deeper insight into the behaviour of the entanglement of formation as a function of T around B_c. Our results are reported in Section III, where we provide the exact mapping between Werner states and the aforementioned thermal states. Finally some conclusions are drawn in Section IV.

II. THE JENSEN-SHANNON DIVERGENCE AND THE ENTROPIC NON-TRIVIALITY MEASURE

We review now a statistical information measure with which we will be concerned in the present work. Let $\vec{P}_{(k)} \in \Omega \subset \mathcal{R}^N$, with $k = 1, 2$, denote two different probability distributions for a particular set of N accessible micro-states. The components of the two probability vectors $\vec{P}_{(k)}$ must satisfy the following two constraints: *a)* $\sum_{j=1}^{N} p_j^{(k)} = 1$, and *b)* $0 \leq p_j^{(k)} \leq 1 \ \forall j$. The set Ω defined by these constraints is the simplex S_N, which is a convex $(N-1)$-dimensional subset of R^N. A quite important, information-theoretical based divergence measure between $\vec{P}_{(1)}$ and $\vec{P}_{(2)}$ was originally introduced by Rao [12] and used by several authors [13]. It came afterwards to be called the Jensen-Shannon divergence (JSD) [14–16] that

- induces a *true* metric in $\Omega \subset \mathcal{R}^N$, being indeed the square of a metric [16], and
- is intimately related to the Kullback-Leibler relative entropy K for two probability distributions $\vec{P}_{(1)}$ and $\vec{P}_{(2)}$, given by [17]

$$K[\vec{P}_{(1)}|\vec{P}_{(2)}] \ = \ \sum_j \ p_j^{(1)} \ \ln\Big(\ p_j^{(1)} \ / \ p_j^{(2)} \ \Big) . \quad (7)$$

We first define

$$J_0[\vec{P}_{(1)}, \vec{P}_{(2)}] = K[\vec{P}_{(1)}|(\frac{1}{2}\vec{P}_{(1)} + \frac{1}{2}\vec{P}_{(2)})], \quad (8)$$

and then the symmetric quantity

$$J_1[\vec{P}_{(1)}, \vec{P}_{(2)}] = J_0[\vec{P}_{(1)}, \vec{P}_{(2)}] + J_0[\vec{P}_{(2)}, \vec{P}_{(1)}] \quad (9)$$
$$= 2S[\frac{1}{2}\vec{P}_{(1)} + \frac{1}{2}\vec{P}_{(2)}]$$
$$- S[\vec{P}_{(1)}] - S[\vec{P}_{(2)}],$$

where $S = -\sum_j p_j \ln p_j$ is the Shannon logarithmic information measure. Let now $\pi_1, \ \pi_2 > 0$; $\pi_1 + \pi_2 = 1$ be the "weights" of, respectively, the probability distributions $\vec{P}_{(1)}, \ \vec{P}_{(2)}$. The JSD reads

$$J^{\pi_1,\pi_2}\left[\vec{P}_{(1)}, \vec{P}_{(2)}\right] = S\left[\pi_1\vec{P}_{(1)} + \pi_2\vec{P}_{(2)}\right] - \pi_1 S\left[\vec{P}_{(1)}\right] - \pi_2 S\left[\vec{P}_{(2)}\right], \quad (10)$$

which is a positive-definite quantity that vanishes iff $\vec{P}_{(1)} = \vec{P}_{(2)}$ almost everywhere [14,15]. In the particular case *to be used in this work*, $\pi_1 = \pi_2 = 1/2$, the measure (10) is symmetric. Notice also that $J^{\frac{1}{2},\frac{1}{2}} = \frac{1}{2}J_1$.

Another statistical tool that we need is the so-called entropic non-triviality measure [18]. The statistical characterization of *deterministic* sources of *apparent* randomness performed by many authors during the last decades has shed much light into the intricacies of dynamical behavior by describing the unpredictability of dynamical systems using such tools as metric entropy, Lyapunov exponents, and fractal dimension [19]. It is thus possible to *i)* detect the presence and *ii)* quantify the degree of deterministic chaotic behavior. Ascertaining the degree of unpredictability and randomness of a system is *not automatically tantamount to adequately grasp the correlational structures that may be present*, i.e., to be in a position to capture the relationship between the components of the physical system. Certainly, the opposite extremes of *i)* perfect order and *ii)* maximal randomness possess no structure to speak of. In between these two special instances a wide range of possible degrees of physical structure exists, degrees that should be reflected in the features of the underlying probability distribution (PD). One would like that they be adequately captured by some functional of PD in the same fashion that Shannon's information measure captures randomness. A candidate to this effect has come to be called the ENTROPIC NON-TRIVIALITY (also, "statistical complexity") $\mathcal{C}$ [18], that should, of course, vanish in the two special extreme instances mentioned above.

In order to illustrate these assertions we can refer to the celebrated logistic map $F : x_n \to x_{n+1}$ [20], where one focuses attention upon the ecologically motivated, dissipative system described by the first order difference equation

$$x_{n+1} = r \ x_n \ (1 - x_n) \quad (\ 0 \leq x_n \leq 1 \ , \ 0 < r \leq 4 \ ) \quad (11)$$

whose dynamical behavior is controlled by r. For values of the control parameter $1 < r < 3$ there exists only a single steady-state solution. Increasing the control parameter past $r = 3$ forces the system to undergo a period-doubling bifurcation. Cycles of period 8, 16, 32, $\cdots$ occur and, if r_n denotes the value of r

where a 2^n cycle first appears, the r_n converge to a limiting value $r_\infty \cong 3.57$ [20]. As r grows still more, a quite rich, and well-known structure becomes apparent. A cascade of period-doubling occurs as r increases, until, at r_∞, the maps becomes chaotic and the attractor changes from a finite to an infinite set of points. For $r > r_\infty$ the orbit-diagram reveals an "strange" mixture of order and chaos, with notable windows of periodicity beginning near $r = 3.83$. As shown in [15], the measure $\mathcal{C}$ is able de give detailed account of the pertinent dynamical features (see, for instance, Figs. 2-4 of [15]).

Typically, the measure $\mathcal{C}$ is the product of two quantities: (1) a normalized entropy (i.e., whose values range between 0 and 1) $H = S/S_{max}$ (the denominator is the largest possible value for S) and (2) a chosen "distance" $d(\vec{P}, \vec{P}_u)$ in probability space that measures "how far" (in this space) the actual PD $\vec{P}$ lies from the *uniform* PD (of maximal entropy) $\vec{P}_u$, i.e.,

$$\mathcal{C} = Hd(\vec{P}, \vec{P}_u) \tag{12}$$

(see, for example, [18,21–26] and references therein). In the present work we are concerned with the probability set (density matrix' eigenvalues) associated to any state ρ and then, with reference to (12), take as H the normalized von Neumann entropy H_{vN} of the relevant state ρ and as d the Jensen-Shannon divergence that will here measure the "distance" from the relevant state to the maximally mixed one ρ_{MM} (proportional to the identity matrix I). Our entropic non-triviality acquires then the aspect (Cf. Eq. (10))

$$C_{JS}(\rho) = J^{1/2,1/2}(\rho, \rho_{MM}) H_{vN}(\rho). \tag{13}$$

One may wonder whether it is possible to built up an entropic non-triviality measure that would depend not on density matrices but directly on wave functions. The concomitant extension is of a rather non trivial nature, but can be accomplished and steps toward its implementation are currently being undertaken. They will be published in the near future.

III. RESULTS

Our main interest refers to the "temperature-evolution" of both C_{JS} and the entanglement of formation E_f as T diminishes, and, eventually, in the limit case $T \to 0$, where a change in the structure of the ground state of hamiltonian (2) is detected for $B_c = 4J_H$. For convenience, we take $J_H = 1$ from now on. In the limit $T \to 0$ one can state that

- 1) $[B < B_c,\ T = 0]$ the ground state (gs) is non-degenerate and equal to the singlet state ($E_f = 1$, $C_{JS} = 0$ for all B)

$$\rho_1^{gs}(T=0) = \begin{pmatrix} 0 & 0 & 0 & 0 \\ 0 & \frac{1}{2} & -\frac{1}{2} & 0 \\ 0 & -\frac{1}{2} & \frac{1}{2} & 0 \\ 0 & 0 & 0 & 0 \end{pmatrix}, \tag{14}$$

- 2) $[B = B_c,\ T = 0]$ the gs state becomes two-fold degenerate, the corresponding two eigenstates being the singlet state *and* $|11\rangle$ ($E_f = E_f^c$, $C_{JS} = C_{JS}^c$)

$$\rho_2^{gs}(T=0) = \begin{pmatrix} 0 & 0 & 0 & 0 \\ 0 & \frac{1}{4} & -\frac{1}{4} & 0 \\ 0 & -\frac{1}{4} & \frac{1}{4} & 0 \\ 0 & 0 & 0 & \frac{1}{2} \end{pmatrix}, \tag{15}$$

- 3) $[B > B_c,\ T = 0]$ the ground state is now $|11\rangle$, which has no entanglement ($E_f = 0$, $C_{JS} = 0$ for all B)

$$\rho_3^{gs}(T=0) = |11\rangle\langle 11| = \begin{pmatrix} 0 & 0 & 0 & 0 \\ 0 & 0 & 0 & 0 \\ 0 & 0 & 0 & 0 \\ 0 & 0 & 0 & 1 \end{pmatrix}. \tag{16}$$

It is clear that, for fixed J_H and at $T = 0$, the entropic no-triviality is zero for all B except for B_c, which is tantamount to asserting that C_{JS} *"detects" the "critical" magnetic strength at which the gs-structure changes.*

We return attention now to the Werner state

$$\rho_W = x|\Phi^+\rangle\langle\Phi^+| + (1-x)\rho_{MM}, \tag{17}$$

where $|\Phi^+\rangle$ is a (maximally entangled) Bell state. This state is unentangled for $x \leq \frac{1}{3}$ [7]. Fig. 1 depicts $C_{JS}(\rho)$ vs. T and $E_f(\rho)$ vs. T for the 1D Heisenberg model in the case $B = 0$. For fixed values of J_H and B, there exists a critical temperature $T_c = \frac{8J_H}{k_B \ln 3}$ above which the system is no longer entangled. The same quantities are depicted in the inset for the Werner state ρ_W. If one considers the plot $C_{JS}(\rho_W)$ vs. $E_f(\rho_W)$ and its thermal Heisenberg counterpart $C_{JS}(\rho)$ vs. $E_f(\rho)$ for $B = 0$, the two graphs coincide. In point of fact, there is a mapping between both states, if we take

$$x = \frac{2}{3}\left[\frac{e^{8\omega} - 3}{1 + e^{-2y} + e^{2y} + e^{8\omega}} + \frac{1}{2}\right], \tag{18}$$

there is a one to one correspondence between the mixed parameter x of the Werner states and the temperature T of the states (3) for each value of $B \leq B_c$ (see Fig. 2) so that x can be regarded as an effective temperature T_{eff}. We remark that

1. at $x = 1$ ($T = 0$) both states are maximally entangled (and have zero complexity) until a critical point is reached,

2. at the critical point $x = \frac{1}{3} \rightarrow T_c = \frac{8J_H}{k_B \ln 3}$ the two states have the same C_{JS}. Notice that all the curves of Fig. 2 (for any several $B-$values) intersect at the point $(x = 1/3, 1/k_B T_c)$,

3. when $x = 0$ $(T \rightarrow \infty)$ both states are unentangled (also with $C_{JS} = 0$).

In the vicinity of B_c, the plots C_{JS} vs. E_f (as parameterized by T) provide a good insight into the ensuing transition mechanism. In Fig. 3 we plot $C_{JS}(\rho)$ vs. $E_f(\rho)$ for several $B-$values near the critical point $B_c = 4$. Note that, as we approach the critical point from either the left (inset) or the right, the entropic non-triviality augments. Pay special attention to the rightwards (B_c^+) approach. We not only appreciate a maximum in C_{JS}, but notice also that E_f is optimal at $B = 4.1$. Thus, maximum C_{JS} equals maximum E_f at the critical point. Vertical and horizontal dashed lines correspond to critical values at $T = 0, B = B_c$. As seen from ρ^{gs}, there is sudden entanglement-change as B crosses $B = B_c$. As C_{JS} can only detect changes in state-structure, its variations can only be produced gs-transitions. Its "transition-detection" feature improves its accuracy in the limit $T \rightarrow 0$.

Transition details near $B_c = 4$ are examined in an even closer fashion in Fig. 4, a C_{JS} vs. E_f plot. We depict things for $B_c^+ = 4.001$ (solid line) and for $B_c^- = 3.99$ (dot-dashed line). Zone I is the region with $E_f > E_f^c$ (B_c^-), wherefrom, as we increase T, the state loses entanglement while increasing its entropic non-triviality (dot-dashed line). See in the inset (solid thick line) the crossing at E_f^c, enhanced in order to appreciate details of the evolution towards maximal entanglement and maximal complexity in the limit $T \rightarrow 0$. On the other hand, if the initial point occurs at B_c^+, no matter whether the temperature changes start at either $T = 0$ or $T = \infty$, we end up at the same $E_f = 0$ point. In particular, for $B = B_c$, there is a single curve that connects the $T = 0$ critical point with the $T \rightarrow \infty$ limit (where $C_{JS} = E_f = 0$). The double-arrow connecting the curves in the two zones illustrates the fact that a path beginning in Zone I (dot-dashed line) cannot smoothly merge with the curve depicted in Zone II (solid line), appearances notwithstanding. A glimpse at the inset clarifies the situation. Vertical and horizontal dashed lines correspond to critical values at $T = 0, B = B_c$.

Fig. 5 is a C_{JS} vs. E_f plot that intends to depict things in the immediate vicinity of the critical point $B_c = 4$. As in Fig. 4, here we fix a very low T (of the order 10^{-3}) while varying B. The solid line corresponds to the entropic non-triviality. See the quasi-circular "motion" around B_c as we decrease the temperature. Inset a) depicts C_{JS} vs. E_f, which, surprisingly, coincides with the "envelope-curve" (Zone I + Zone II) of Fig. 4. This remarkable fact can be explained because in Fig. 4 both the "upper" branch of the curves in Zone I *and* the curve of Zone II are drawn for low T-values nearby $B = Bc$. Since here we "sit" at the critical point (and very low temperatures are used) both curves of inset a) look like a continuous lines. In other words, only a low $B-$range of values around B_c is relevant at such low temperatures. Inset b) depicts the behavior of the degree of mixture $R = 1/Tr[\rho(T)^2]$ vs. E_f. In the limit $T \rightarrow 0$, R reaches $R = 2$, as expected. Vertical and horizontal dashed lines correspond to critical values at $T = 0, B = B_c$.

IV. CONCLUSIONS

In this paper we have shown that the Jensen-Shannon entropic non-triviality measure C_{JS} is able to detect the "critical" magnetic strength at which the gs-structure changes. Also, via C_{JS} we discover that there is a one to one correspondence between Werner states and the Heisenberg anti-ferromagnet for values of $B \leq B_c$. As shown in Fig. 2, it is possible to assign to the mixing Werner parameter x an effective temperature T_{eff} for each value of $B \leq B_c$. Finally, the physics in the immediate vicinity of the critical point $B_c = 4$ can be analyzed in detailed fashion using C_{JS}. In the one dimensional Heisenberg model, for two spinors, maximum entanglement implies maximum entropic non-triviality in the vicinity of the corresponding critical point.

Acknowledgements

This work was partially supported by the MEC grant BFM2002-03241 (Spain) and FEDER (EU), by the Government of Balearic Islands and by CONICET (Argentine Agency).

FIGURE CAPTIONS

Fig. 1- Evolution of (1) the entanglement of formation E_f and (2) the Jensen-Shannon complexity C_{JS} vs. the temperature T for the thermal state $\rho(T)$ of two-qubits in the 1D Heisenberg model. For given values of J_H and B there exists a critical temperature $T_c = \frac{8J_H}{k_B \ln 3}$ above which the system is no longer entangled. The same quantities are depicted in the inset for the Werner state ρ_W. There is a one to one mapping between both type of states for $B \leq B_c$. See text = for details.

Fig. 2- Mapping of the mixed Werner parameter x as a function of $1/T$ for several values of B. The horizontal lines correspond to $x = 1/3$ and $x = 2/3$, respectively.

Fig. 3- Plot of the complexity C_{JS} vs. the entanglement of formation E_f near the critical point $B_c = 4$. As we approach the critical point from either left (inset) or right, the complexity augments. In the B_c^+ case we not only

have a maximal C_{JS}, but also an optimal E_f. Vertical and horizontal dashed lines correspond to critical values at $T = 0, B = B_c$. See text for details.

Fig. 4- Same as before, but with additional details. We have $B_c^+ = 4.001$ (solid line) and $B_c^- = 3.99$ (dot-dashed line). Zone I (II) denotes the region with $E_f > E_f^c$ and B_c^- ($E_f < E_f^c$ and B_c^+). In the inset the crossing region at E_f^c is enhanced in order to see how details of the evolution around maximum entanglement and maximum complexity in the limit $T \to 0$. See text for details.

Fig. 5- Plot of the complexity C_{JS} in the vicinity of the critical point $B_c = 4$. The inset a) depicts C_{JS} vs. E_f, which, surprisingly, coincides with the enveloping curve (Zone I + Zone II) of Fig. 3. Inset b) depicts the behaviour of the degree of mixture $R = 1/Tr[\rho(T)^2]$ vs. E_f. In the limit $T \to 0$, R reaches the value $R = 2$, as expected. Vertical and horizontal dashed lines correspond to the critical values at $T = 0, B = B_c$. See text for details.

[1] H.-K. Lo, S. Popescu, T. Spiller (Eds.), Introduction to Quantum Computation and Information, (World Scientific, River Edge, 1998).
[2] C. P. Williams, S. H. Clearwater, Explorations in Quantum Computing, (Springer, New York, 1997).
[3] C. P. Williams (Ed.), Quantum Computing and Quantum Communications, (Springer, Berlin, 1998).
[4] D. Bouwmeester, A. Ekert, A. Zeilinger (Eds.), The Physics of Quantum Information, (Springer, Berlin, 1998).
[5] G. Alber, T. Beth, P. Horodecki, R. Horodecki, M. Röttler, H. Weinfurter, R. Werner, A. Zeilinger, Quantum Information, Springer Tracts in Modern Physics, Vol. 173, Berlin, 2001.
[6] G. P. Berman, G. D. Doolen, R. Mainieri, V. I. Tsifrinovich, Introduction to Quantum Computers, (World Scientific, Singapur, 1998).
[7] R. F. Werner, Phys. Rev. A **40** (1989) 4277.
[8] S. Popescu, Phys. Rev. Lett **72** (1994) 797.
[9] S. Popescu, Phys. Rev. Lett. **74** (1995) 2619.
[10] C. H. Bennett, G. Brassard, C. Crepeau, R. Jozsa, A. Peres, W. K. Wootters, Phys. Rev. Lett. **70** (1993) 1895.
[11] M. C. Arnesen, S. Bose, and V. Vedral, Phys. Rev. Lett. **87** (2001) 017901.
[12] C.R. Rao, *Differential Geometry in Statistical Inference* (IMS-Lecture Notes, Vol. 10, 1987, pp. 187)
[13] J. Lin, IEEE Trans. Inf. Theory **37** (1991) 1.
[14] I. Grosse, P. Bernaola-Galvan, P. Carpena, R. Román-Roldán, J. Oliver, H. E. Stanley. Phys. Rev. E **65** (2002) 41905.
[15] P. W. Lamberti, M. T. Martin, A. Plastino, and O. A. Rosso, Physica A **334** (2004) 119.
[16] F. Topsoe, Preprint University of Copenhagen (2002).
[17] S. Kullback and R. A. Leibler, Ann. Math. Stat. **22** (1951) 79.
[18] P.W. Lamberti, M.T.Martin, A. Plastino, and O.A. Rosso, Physica A **334** (2004) 119.
[19] C. Beck and F. Schlögl, *Thermodynamic of chaotic systems* (Cambridge University Press, NY, 1993).
[20] E. Ott, T. Sauer, and J. A. Yorke, *Coping with chaos* (John Wiley & Sons, Inc, NY, 1994).
[21] R. López-Ruiz, H. L. Mancini and X. Calbet, Phys. Lett. A **209** (1995) 321.
[22] C. Anteneodo and A. R. Plastino, Phys. Lett. A **223** (1997) 348.
[23] X. Calbet and R. López-Ruiz, Phys. Rev. E **63** (2001) 066116.
[24] S. H. Shiner, M. Davison, and P. T. Landsberg, Phys. Rev. E **59** (1999) 1459.
[25] M. T. Martin, A. Plastino, and O. A. Rosso, Phys. Lett. A **311** (2003) 126.
[26] O. A. Rosso, M. T. Martin, and A. Plastino, Physica A **320** (2003) 497.

fig.1

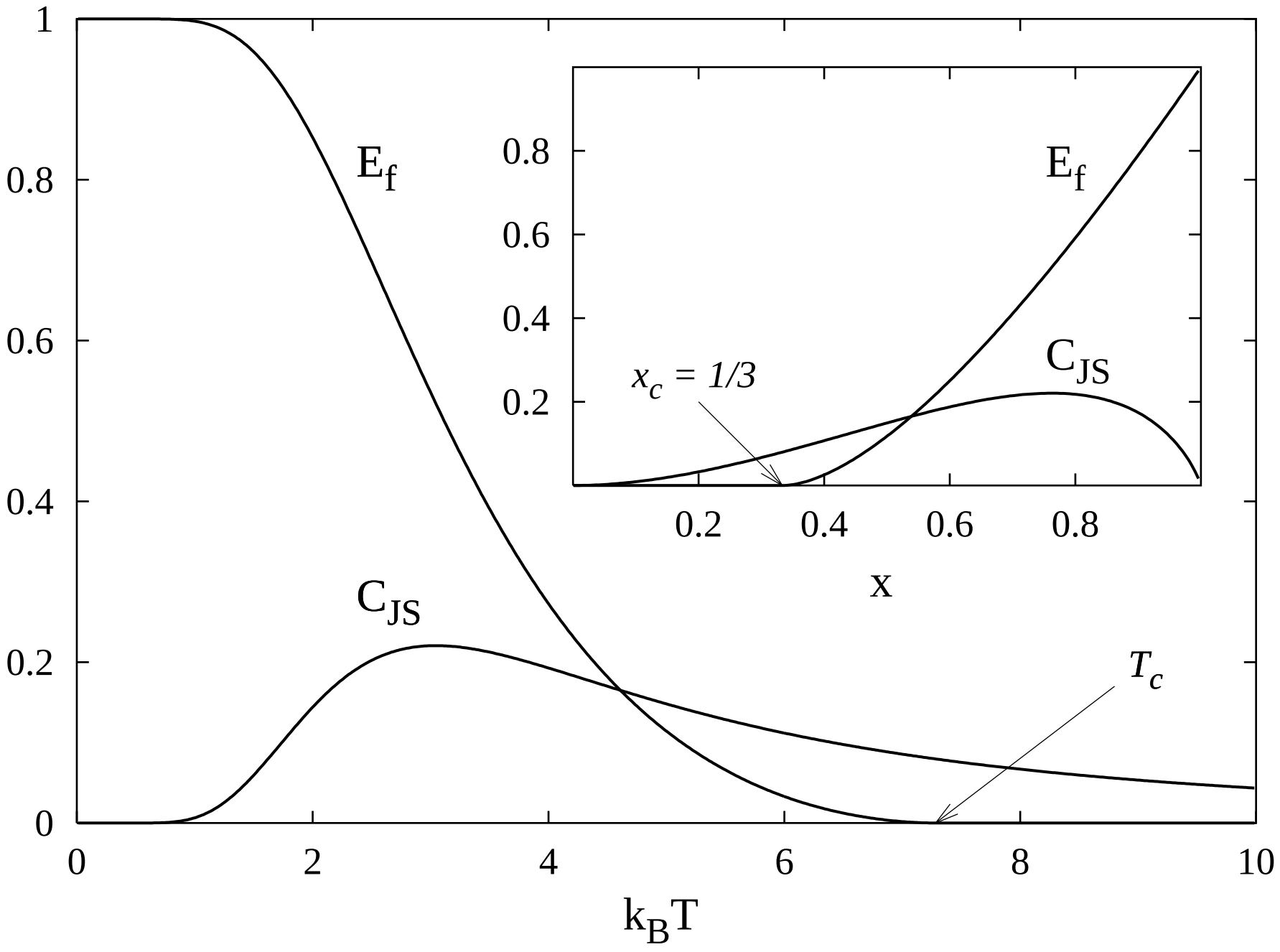
1
0.8
0.6
0.4
0.2
0
0
2
4
6
8
10
k_BT
E_f
C_{JS}
T_c
0.8
0.6
0.4
0.2
E_f
C_{JS}
x_c = 1/3
0.2
0.4
0.6
0.8
x

fig.2

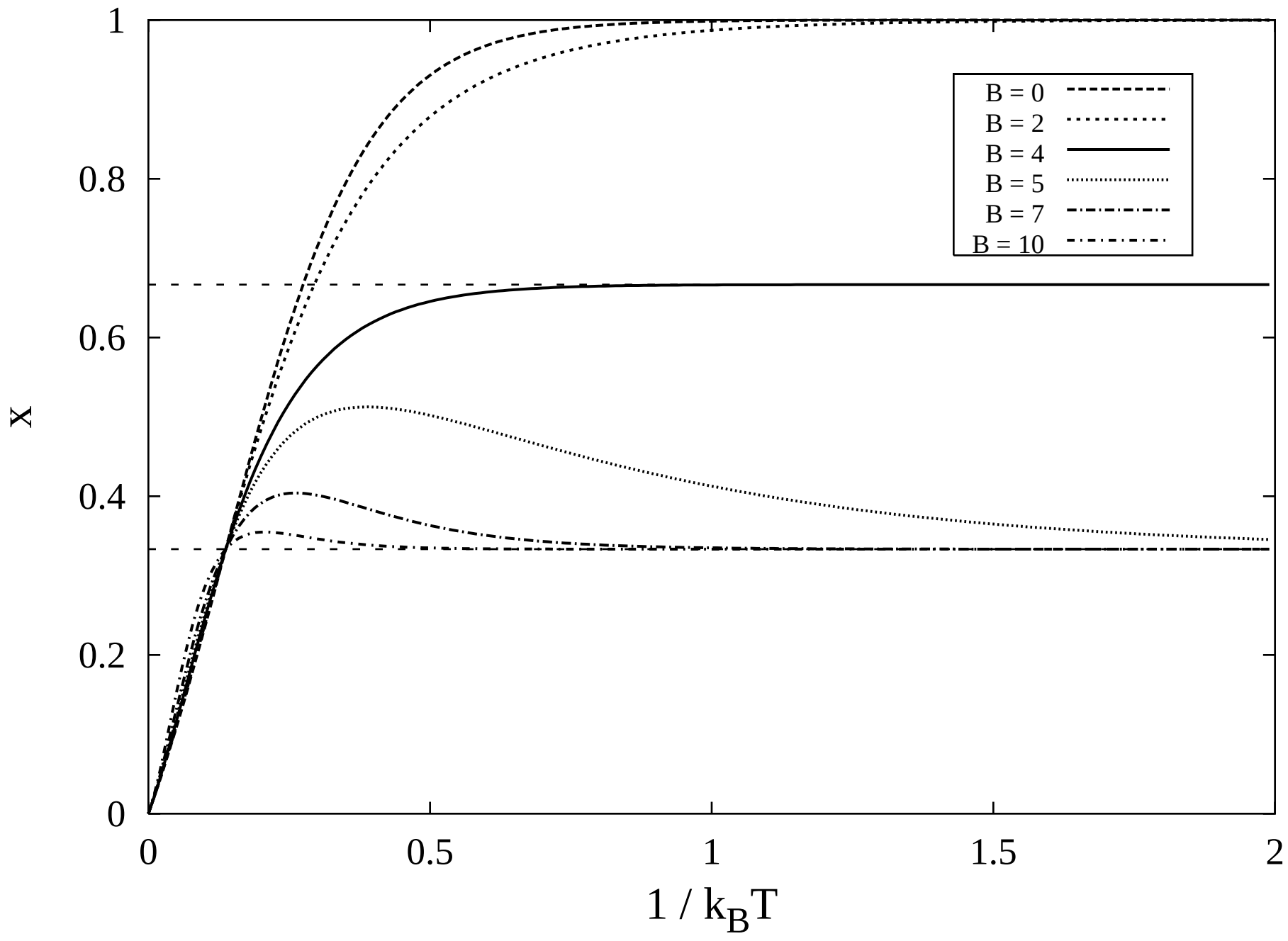

fig.3

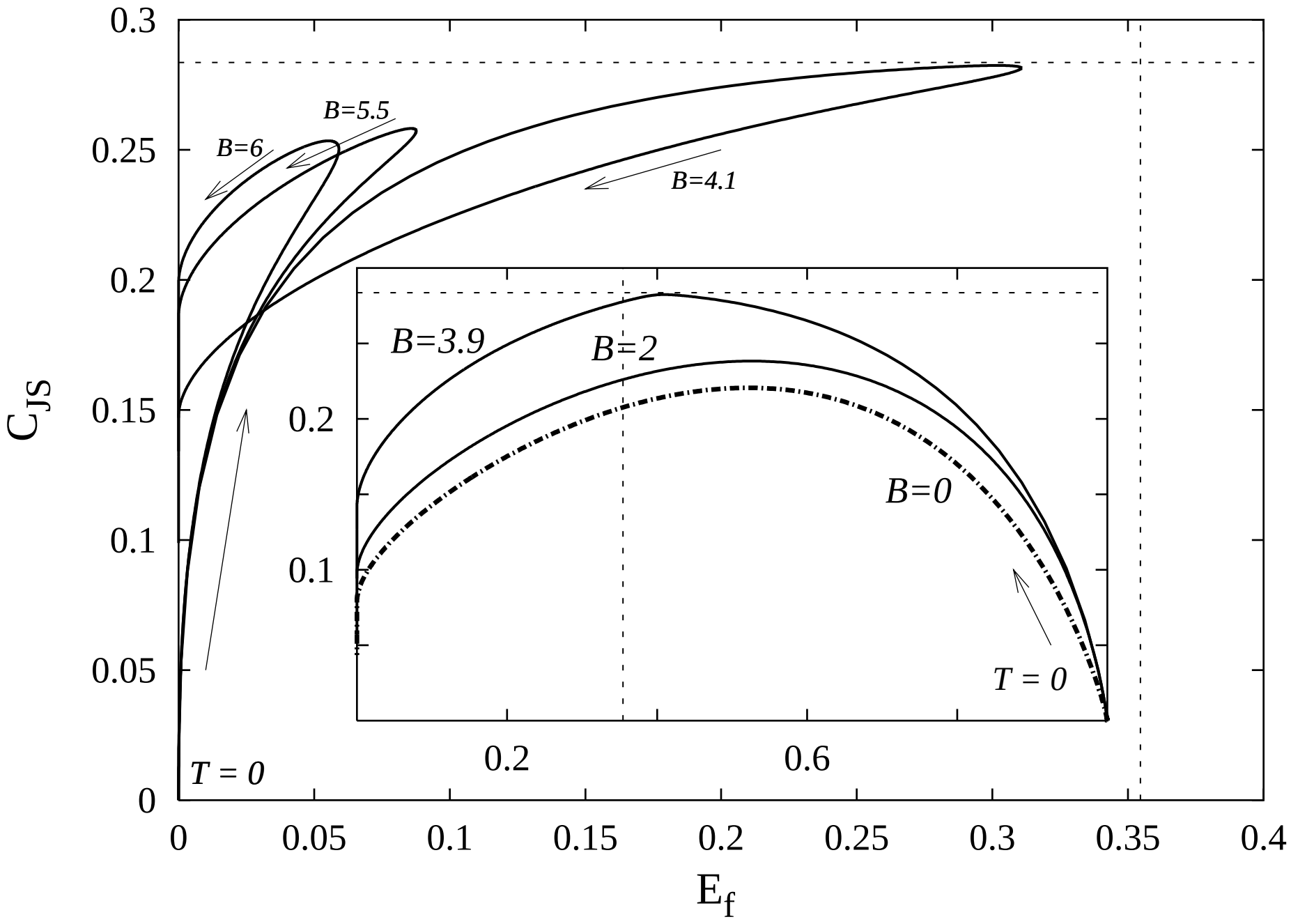
0.3
0.25
0.2
0.15
0.1
0.05
0
0
0.05
0.1
0.15
0.2
0.25
0.3
0.35
0.4
C_{JS}
E_f
B=5.5
B=6
B=4.1
T = 0
B=3.9
B=2
B=0
T = 0
0.2
0.1
0.2
0.6

fig.4

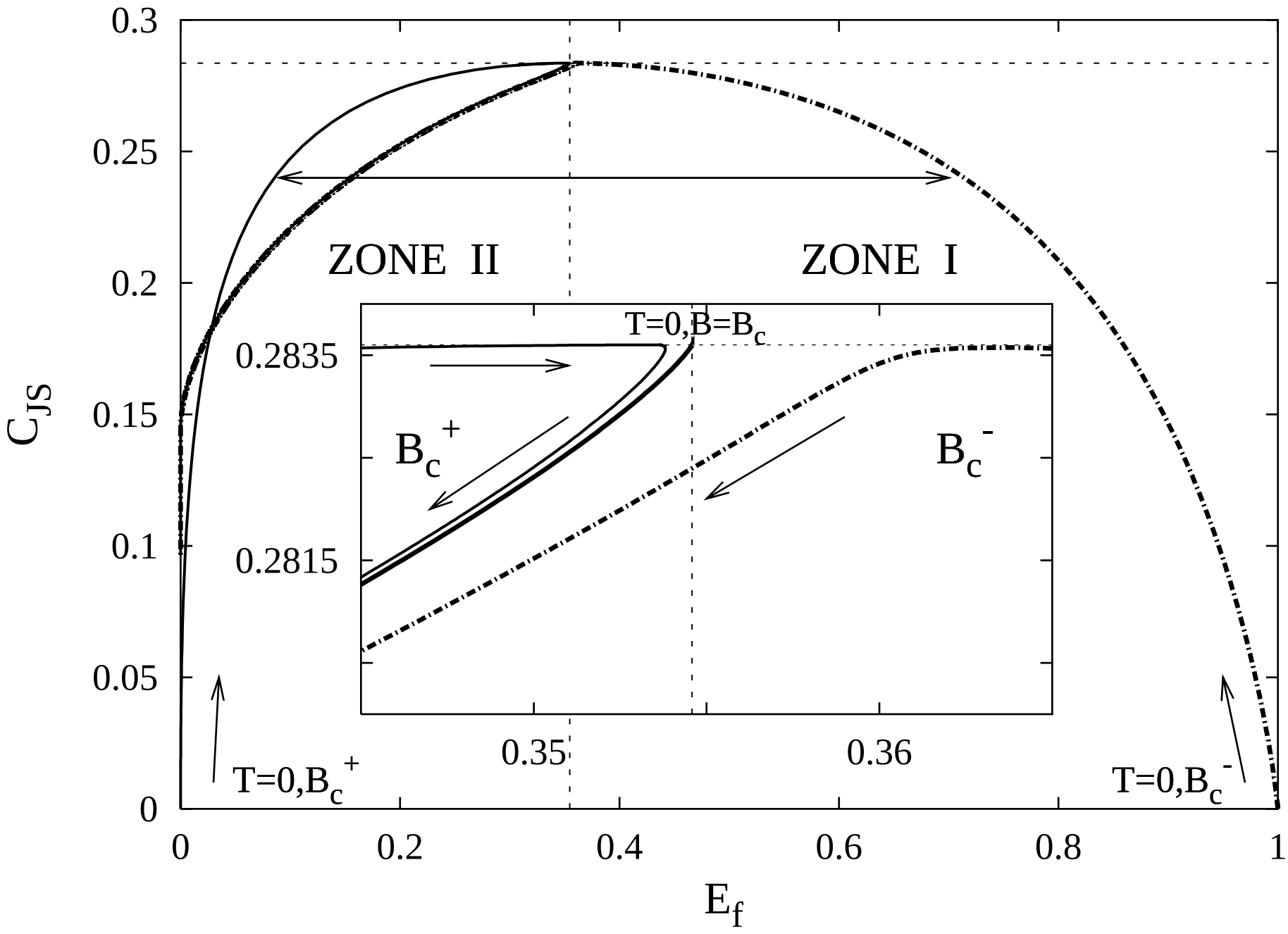
0.3
0.25
0.2
0.15
0.1
0.05
0
0
0.2
0.4
0.6
0.8
1
C_{JS}
E_f
ZONE II
ZONE I
T=0,B=B$_c$
0.2835
0.2815
B$_c^+$
B$_c^-$
0.35
0.36
T=0,B$_c^+$
T=0,B$_c^-$

fig.5

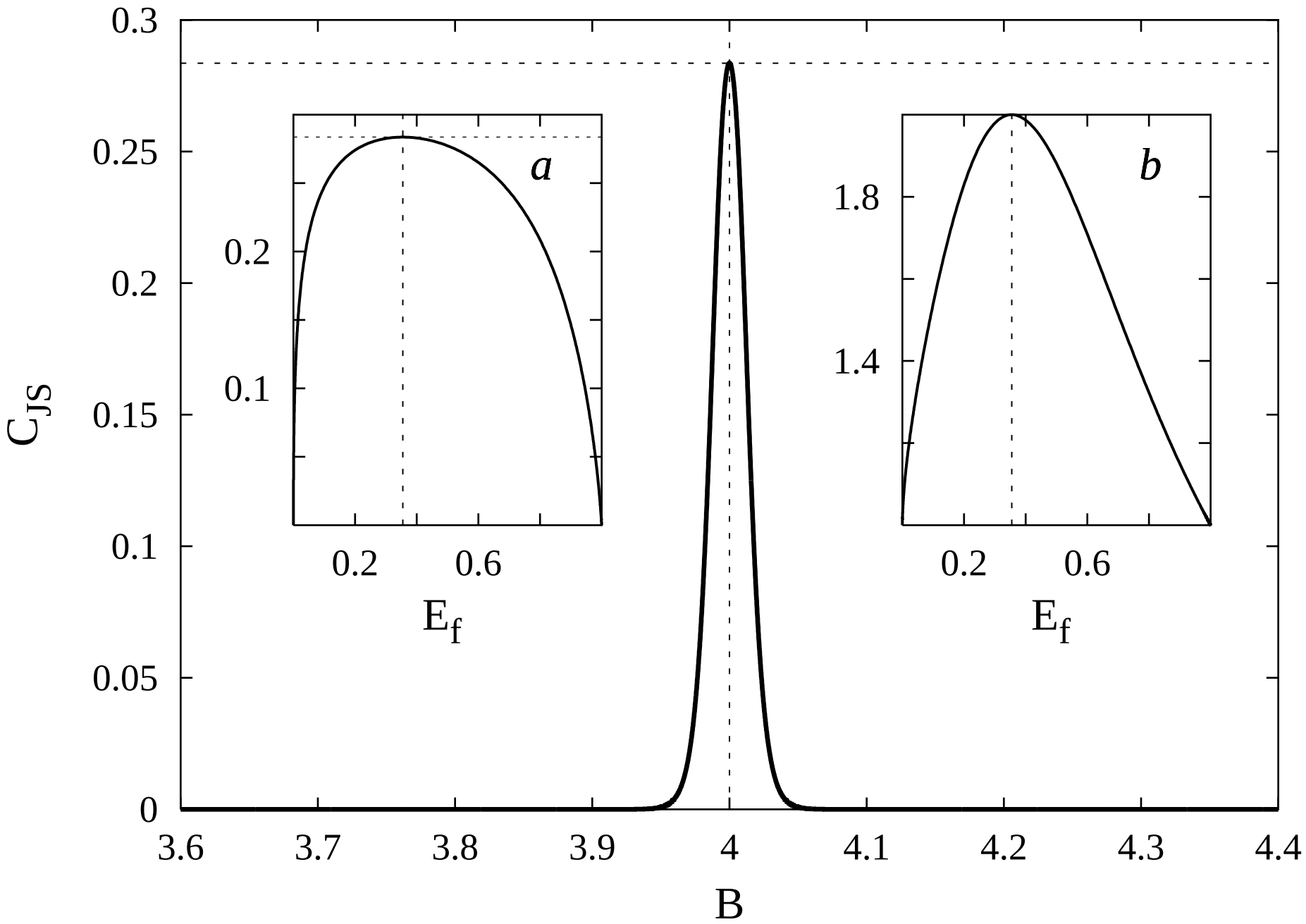
0.3
0.25
0.2
0.15
0.1
0.05
0
C_{JS}
3.6
3.7
3.8
3.9
4
4.1
4.2
4.3
4.4
B
a
0.2
0.1
0.2
0.6
E_f
b
1.8
1.4
0.2
0.6
E_f